

Spectroscopy and Single-Molecule Emission of a Fluorene-Terthiophene Oligomer

G. E. Khalil,^{†,‡,⊥} A. M. Adawi,^{†,‡} B. Robinson,[†] A. J. Cadby,[†] W.C. Tsoi,[§] J-S. Kim,[§] A. Charas,^{||} J. Morgado,^{||} and D. G. Lidzey^{*,†}

[†]Department of Physics and Astronomy, University of Sheffield, Hicks Building, Hounsfield Road, Sheffield S3 7RH, United Kingdom

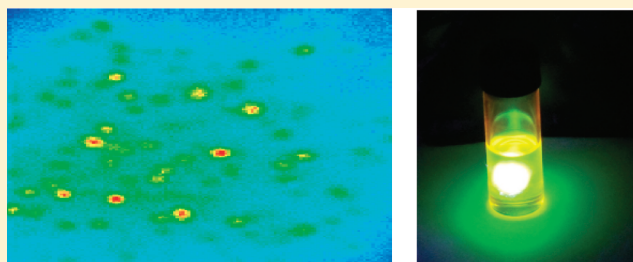
[‡]National Institute of Laser Enhanced Science (NILES), Cairo University, Cairo, Egypt

[§]The Blackett Laboratory, Imperial College, Prince Consort Road, London SW7 2BZ, United Kingdom

^{||}Instituto de Telecomunicações, Av. Rovisco Pais, P-1049-001 Lisboa, Portugal

S Supporting Information

ABSTRACT: We study the thiophene-based oligomer poly[2,7-(9,9-bis(2'-ethylhexyl)fluorene)-alt-2,5-terthiophene] (PF3T) in solution and when dispersed at low concentration into a polynorbornene matrix. We find that at high concentration in solution the 0–0 electronic transition observed in fluorescence is suppressed, a result indicative of the formation of weakly coupled H-aggregates. At low concentration in a polymer matrix, emission from both single molecules and molecular aggregates is observed. We find that the fluorescence spectra of most PF3T emitters are composed of a number of relatively narrow emission features, indicating that the emission usually occurs from multiple chromophores. A small number of PF3T molecules are however characterized by single chromophore emission, spectral blinking, and narrowed emission peaks.



I. INTRODUCTION

Interest in semiconducting conjugated polymers is driven by their applications in molecular optoelectronic devices such as organic light emitting diodes,¹ organic field-effect transistors,² solar cells,³ and biological and chemical sensors.⁴ One important property of these materials is that their optical and electronic properties can be tuned by chemical modification. The polyfluorene family of conjugated polymers is one of the most important examples of such materials. Within this family, fluorene units are copolymerized with other conjugated moieties to modify their optical and electronic properties such as electron affinity (EA) and ionization potential (IP).^{5–8} One example of such a copolymer is the polymer poly[2,7-(9,9-bis(2'-ethylhexyl)fluorene)-alt-2,5-terthiophene] (PF3T). Here the copolymerization of 9,9-bis(2'-ethylhexyl)fluorene with terthiophene shifts the blue fluorene emission to longer (orange/red) wavelengths.

In this paper, we report a study of a low mass sample of the statistical oligomer poly[2,7-(9,9-bis(2'-ethylhexyl)fluorene)-alt-2,5-terthiophene] (PF3T), whose synthesis, characterization, and singlet and triplet state properties have previously been reported.^{5–10} Here, we propose that this material forms weakly interacting H-aggregates at high concentration in both thin-film and solution. This aggregation process has been previously studied both theoretically and experimentally in the polymer poly(3-hexylthiophene) P3HT.^{11–13} Here, due to the extended conjugation length of the polymer, it has been proposed that Coulombic coupling between neighboring molecules is smaller

than the vibrational relaxation energy, with intermolecular interaction leading to the splitting of the vibronic sublevels.¹³ In such weakly coupled aggregates, transitions to and from the electronic ground state to the lowest energy state of the 0–0 band has zero oscillator strength. As energetic relaxation occurs from this lowest energy level to the ground-state, the fluorescence from the purely electronic 0–0 transition is not permitted. Direct absorption from the ground state to the top of the 0–0 band is however still permitted. Due to disorder, the suppression of the 0–0 transition is not complete but simply weakened. This has been shown to provide a good description of the PL emission spectra of P3HT in which the 0–0 transition becomes stronger as the solution concentration is decreased.¹³ Here, we observe a very similar set of phenomena in the related material PF3T and show that, at sufficiently low concentration, PF3T aggregation is relatively suppressed with the 0–0 electronic transition dominating the fluorescence emission. We also use single-molecule spectroscopy techniques to study PF3T, and identify both single and multiple chromophore emission together with spectral “blinking”.

II. EXPERIMENTAL METHODS

The chemical structure of the PF3T used in this study is shown in Figure 1. The material studied had a molecular weight of

Received: July 6, 2011

Revised: September 13, 2011

Published: September 14, 2011

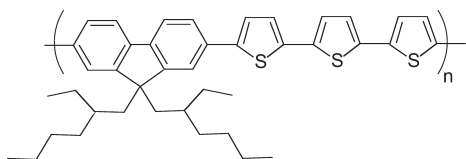


Figure 1. Chemical structure of PF3T.

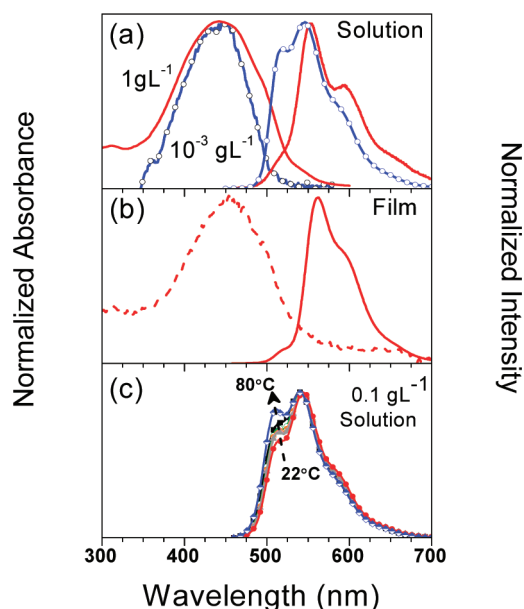


Figure 2. Normalized absorption and fluorescence spectra of (a) 1 g L^{-1} (red-line) and 10^{-3} g L^{-1} (blue-line) solutions of PF3T in toluene, (b) a thin PF3T film spin-cast from a 1 g L^{-1} solution. Part (c) shows the temperature dependent PL emission from PF3T in a toluene solution at a concentration of 0.1 g L^{-1} .

4.2 kDa and polydispersity (M_w/M_n) = 1.5, corresponding to approximately 4–5 monomer units¹ or 20–25 phenyl/thiophene rings. Solution absorption and fluorescence spectra were recorded on Horiba Jobin Yvon Fluoromax-4 spectrofluorometer, which covered a spectral range of 200–1000 nm. We have also characterized Raman scattering from both PF3T thin films and the polynorbornene (Zeonex) matrix in which they were dispersed using a Renishaw Raman microscope equipped with a He:Ne laser operating at 632.8 nm. The fluorescence decay lifetime of PF3T thin films and solutions was also measured at a series of different emission wavelengths. Here, films were excited using laser pulses from a 80 MHz frequency doubled mode-locked Ti:sapphire laser at 380 nm. Luminescence was detected using a Hamamatsu R3809U multichannel-plate photomultiplier tube in photon counting mode, with pulses fed to a Becker and Hickl time-correlated photon counting system (TCSPC) having a temporal resolution of ~ 70 ps.

Samples for single-molecule spectroscopy (SMS) were prepared by spin-casting a toluene solution containing PF3T at a concentration between 0.01 and $0.1 \mu\text{g L}^{-1}$ and Zeonex at a concentration of 20 mg/mL onto a silver mirror substrate to form a film of 80 nm thickness. For spectroscopic measurements, each film was mounted into a continuous flow, coldfinger helium cryostat held at 4 K under a vacuum better than 10^{-5} mbar. A He: Cd laser (442 nm) was then used to generate fluorescence from the film as described previously.¹⁴ A home-built wide-field

microscope was used to image the fluorescence from the film, with a series of isolated emitting “spots” having a typical surface density $0.01 \mu\text{m}^{-2}$ observed. Absorption anisotropy of such emitting spots was measured by rotating the polarization of the excitation laser using a half-wave-plate while recording the spectrally integrated emission as a function of polarization angle θ . We have also studied time-dependent emission from emitters under continuous-wave excitation to evidence blinking (a characteristic feature of isolated chromophores). Here, a series of images were recorded every 50 ms using a Princeton Instruments PRO-EM Electron Multiplied CCD camera, permitting us to extract the time-dependent emission intensity of each emitter.

III. RESULTS AND DISCUSSION

A. Thin Film and Solution Spectroscopy of PF3T. Figure 2 shows the absorption and fluorescence emission of the PF3T oligomer studied at room temperature when prepared in the form of a thin film and when dissolved in solution. Specifically, Figure 2a shows measurements made on a PF3T toluene solution at two different concentrations (10^{-3} and 1 g L^{-1}), with Figure 2b showing absorption and fluorescence of a 30 nm thick film spin-cast from toluene. In solution at a concentration of 10^{-3} g L^{-1} , the absorption peaks at 445 nm. As the solution concentration is increased to 1 g L^{-1} the absorption band broadens and a distinct shoulder appears around 510 nm. In a 10^{-3} g L^{-1} solution, we find that the fluorescence emission is characterized by peaks at 507, 547, 595, and 652 nm. At a concentration of 1 g L^{-1} , the fluorescence intensity of the emission is reduced significantly, with the emission peak observed at 507 nm becoming significantly weaker. Notably, the emission and absorption spectra of the 1 g L^{-1} concentration solution is similar to that of the thin-film (see Figure 2b).

Previous work has shown that the intensity of the 0–0 emission peak in a conjugated polymer can be reduced by self-absorption (an internal filter effect) owing the overlap of the absorption and emission spectra.¹⁵ While we do not discount that there is a small degree of self-absorption in PF3T films and solutions studied here, we do not believe that this adequately accounts for the relative weakness of the emission peak observed at 507 nm. We are confident in this assertion as the PL spectra emitted by films having a thickness significantly less than 30 nm (in which the optical density at 507 nm is very small) are very similar to those presented in Figure 2b. We therefore conclude that the reduction in emission intensity at 507 nm results from enhanced intermolecular interactions in higher concentration solutions and in thin-films. To determine the effect of intermolecular interactions in modifying the emission spectrum of PF3T, we have recorded PL emission spectra from a 0.1 g L^{-1} PF3T solution as it is cooled from 80 °C to room temperature. This is plotted in Figure 2c with all spectra normalized to the emission peak at 547 nm. It can be seen that as the temperature of the PF3T solution is reduced, the emission peak at 507 nm becomes relatively weaker.

A similar effect has been observed by Clark et al in the polymer poly(3-hexylthiophene) [P3HT]¹³ and was ascribed to the formation of H-aggregates resulting from Coulombic interactions between closely packed π -stacked molecules. In such weakly coupled H-aggregates, transitions from the first excited state to the ground-state are dipole forbidden, with the 0–0 emission transition being dark while other transitions to vibrationally excited ground-states remaining dipole-allowed. As we argue here, we believe a similar picture is applicable in the material PF3T.

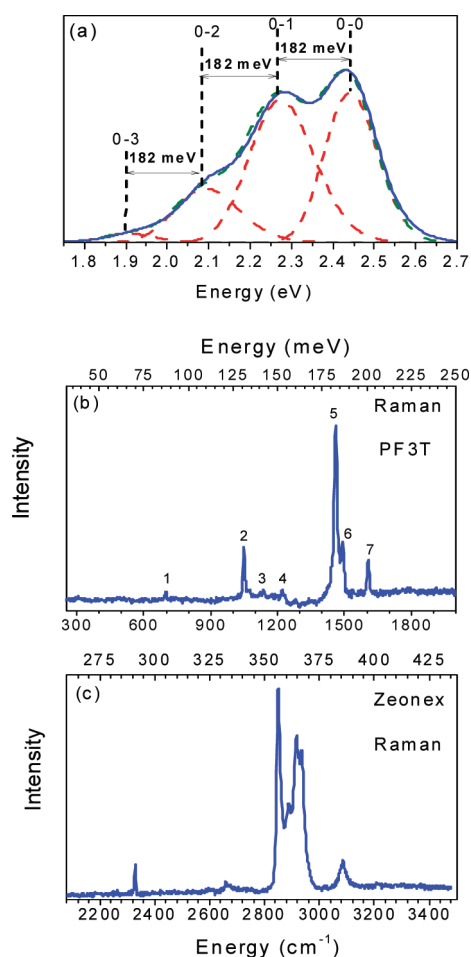


Figure 3. Part (a) shows an ensemble emission spectrum recorded from a large area of the PF3T film surface when dispersed in a Zeonex matrix at a concentration of $0.5 \mu\text{g L}^{-1}$. Here the spectrum is fitted with a series of Gaussian functions that identify 0–0, 0–1, 0–2, and 0–3 transitions. Raman spectra of (b) PF3T and (c) Zeonex (recorded using a 632.8 nm excitation).

Indeed, work on a series of related compounds (polyfluorene-bithiophene oligomers) has evidenced the formation of monodomain glassy-nematic films indicative of strong self-ordering between molecular backbones.¹⁶ Such ordering leads to significant electronic interactions between neighboring molecules, with a theoretical and spectroscopic study on a series of light-emitting nematic liquid crystals based on fluorene and thiophene moieties¹⁷ highlighting the formation of both J- and H-aggregates dependent on the relative longitudinal displacement of neighboring molecules. Aggregation-induced spectral changes have also been observed in the polymer MEH-PPV,^{18,19} where the emergence of structural order that forms supramolecular assemblies is correlated with a red-shift of both optical absorption and fluorescence emission. Indeed, the weakness of the 0–0 transition in 2,5-diheptyloxy substituted phenylene vinylene oligomers has been interpreted in terms of the formation of H-aggregates.²⁰ We note however the luminescence spectra of poly(*p*-phenylenevinylene) [PPV] and substituted PPVs have also been explained in terms of emission from both molecular excitons and lower-lying interchain states.²¹

To determine whether an H-aggregate model is appropriate to understand the concentration dependence of PF3T emission, it is first necessary to clarify the origin of the various peaks observed in the PF3T fluorescence spectra. We have therefore recorded

the fluorescence emission from PF3T in a low concentration solution ($5 \times 10^{-7} \text{ g L}^{-1}$) to eliminate most of aggregation effects evidenced in Figure 2a. This is shown in Figure 3a, where it can be seen that the PL emission is fit using four Gaussian functions. This Gaussian fitting allow us to identify peaks at 507 nm (2.442 eV), 547 nm (2.265 eV), 595 nm (2.082 eV), and 652 nm (1.903 eV), with peaks having a line width of 145, 175, 184, and 147 meV, respectively. We can identify the origin of such features by reference to a Raman spectrum recorded from a PF3T thin-film when cast on a silver mirror as shown in Figure 3b. Here a series of modes are observed the origin of which we identify in Table 1.

It can be seen that the dominant feature observed in the Raman scattering spectrum is the mode at 182 meV (the symmetric C=C stretch mode in the thiophene-ring). As has been observed in P3HT,²³ the electronic transition of PF3T couples strongly to this mode, with the energy between each of the peaks observed in the low-concentration fluorescence spectra being separated in energy by approximately 182 meV (see Figure 3a). We propose therefore that the emission feature observed at 507 nm corresponds to the 0–0 (electronic) transition, with peaks at 547, 595, and 652 nm corresponding to 0–1, 0–2, and 0–3 vibronic transitions.

To explore the effect of molecular aggregation, we have recorded the PL emission from PF3T as a function of concentration in solution and in a matrix and as a function of the excitation wavelength.³⁰ In Figure 4a, we plot the emission from PF3T dissolved in a toluene solution as a function of concentration ranging from 1 g L^{-1} to 5 ng L^{-1} recorded at room temperature. In parts b and c, we plot the bulk emission from thin films of PF3T dispersed in a Zeonex matrix at 20 mg L^{-1} when cast from a solution at concentrations ranging from 1 g L^{-1} to $0.05 \mu\text{g L}^{-1}$ recorded at room temperature (part b) and 4 K (part c). Note, all spectra in parts a and c have been normalized relative to their 0–1 peak emission intensity, whereas in part b data has been normalized to the peak emission intensity. It can be seen that for both solution and thin-films, the intensity of the 0–0 electronic transition increases as the concentration of PF3T is reduced with other features (vibronic replicas) undergoing a progressive blue-shift. This suggests that at high concentration, molecular aggregation and solid-state packing induces a general increase in average electronic conjugation length and also suppresses the 0–0 transition as observed in P3HT.¹³ It has been argued that in the polymer P3HT, emission from the 0–0 transition is not completely suppressed due to disorder, however is simply weakened.¹³ We anticipate a similar effect here, however we believe the fluorescence spectra presented in Figure 4 reflects emission from both single molecules and also molecules that have undergone aggregation. In Figure S1, we plot the Huang–Rhys factor (*S*) for the spectra presented in Figure 4a–c as a function of PF3T concentration. These were calculated³¹ on the basis of the relative peak intensity of the assumed 0–0 and 0–1 transitions using the relation $I_{0 \rightarrow n}/I_{0 \rightarrow 0} = S^n/n!$. Note however that it has been shown that the absorption and emission spectra of P3HT thin-films cannot be fit using a simple Franck–Condon progression,¹³ and so this analysis must be treated with caution. Nevertheless, this approach permits us to quantify the change in emission spectra, with, for example, the Huang–Rhys factor changing from 7.8 in a 10^6 mg L^{-1} PF3T solution to 0.65 in a 5 ng L^{-1} solution. A similar change in Huang–Rhys parameter is also determined in diluted thin film. It is also apparent that the intensity of the various transitions in the emission spectra have some temperature dependence; an effect that we discuss below.

Table 1. Assignment of Raman Modes Observed in PF3T

no.	mode energy (meV)	origin	refs
1	79	C–S–C ring deformation	22 and 23
2	127	C–H in-plane bending of the thiophene rings	22
3	142	C–H in-plane bending (wagging) of the phenylene rings	23–27
4	153	inter-ring C–C stretching	23, 27, and 28
5	182	symmetric C=C stretching mode in the aromatic thiophene ring	22, 23, 25, and 27
6	187	an antisymmetric C=C stretch	22, 23, 25
7	206	symmetric phenylene ring stretching mode	24, 26, and 29

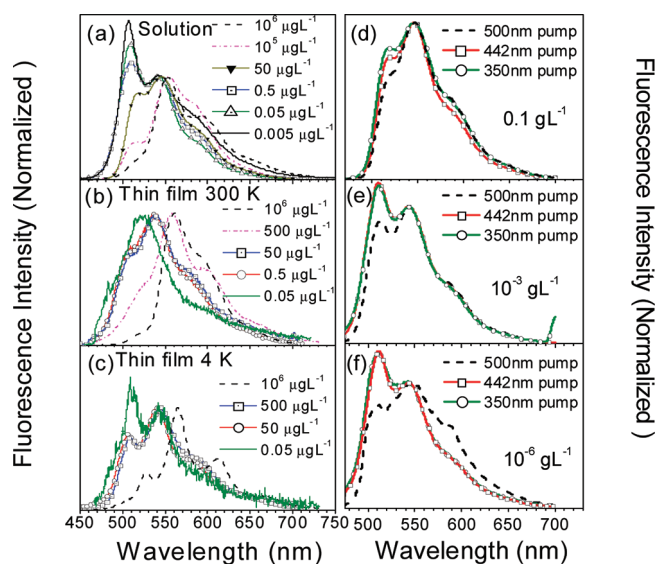


Figure 4. Series of ensemble PL emission spectra recorded from PF3T when dispersed (a) in a toluene solution at different concentrations and (b) and (c) in a Zeonex matrix at different concentration at room temperature and 4 K respectively. Parts d–f show PL emission as a function of excitation wavelength for PF3T in a toluene solution at a concentration of 0.1, 10^{-3} , and 10^{-6} g L $^{-1}$, respectively.

We now return to the absorption spectra shown in Figure 2a. Previous studies on the polymer P3HT have shown that as molecules extend and planarize as a thin film undergo crystallization, the absorption spectrum undergoes a spectral red-shift with the appearance of a more clearly resolvable vibronic transitions.³² This change in optical properties reflects a molecular system in which the average electronic conjugation length of molecules increases with increased structural ordering and improved molecular packing, thereby reducing inhomogeneous broadening. We propose therefore that the red-shifted shoulder observed in the PF3T absorption spectra recorded from higher concentration solutions (see Figure 2a) is the partially resolvable 0–0 electronic transition of molecules that have some degree of extended conjugation as a result of nanoscale aggregation or intermolecular packing.

We can test this hypothesis by recording PL emission spectra from PF3T at different concentration in solution and at three different excitation wavelengths (350, 442, and 500 nm) as shown in Figures 4d–f. As can be seen, as the solutions are excited at longer wavelengths, the relative intensity of the 0–0 transition is reduced. This effect becomes increasingly pronounced in lower concentration solutions. This suggests that long-wavelength excitation more effectively selects molecules

with increased electronic conjugation, confirming that the red-shifted absorption (evidenced in Figure 2a) is associated with molecular aggregation. Excitation at shorter-wavelengths (350 and 442 nm) however preferentially excites unaggregated molecules with the 0–0 emission being substantially stronger. Note, that this dependence on excitation wavelength becomes more pronounced as concentration is reduced. We propose that in high concentration solutions, energy transfer via dipole–dipole coupling (Förster transfer) more effectively allows excitons to seek out aggregated molecules having extended conjugation length and thus lower energy, adequately explaining this effect.

The migration of excitons between unaggregated and aggregated molecules also permits us to understand the temperature dependence of fluorescence emission recorded from ‘dilute’ thin films at room temperature (Figure 4b) and at 4 K (Figure 4c). Here, it can be seen that the 0–0 emission peak in the higher concentration films appears relatively stronger at lower temperature. This can also be more clearly seen in the temperature dependent PL emission spectra shown in Figure S2. This effect is not expected in the context of the H-aggregate model discussed above, as increased temperature should lead to increased disorder which will help to populate states higher in the band, thus increasing the intensity of the 0–0 peak at higher temperatures. We can however explain this discrepancy on the basis of exciton-diffusion. It has been shown that as temperature is reduced, exciton diffusion in a disordered organic-semiconductor film becomes increasingly hindered³³ as it has a thermally activated component. We speculate therefore that in the thin films studied, only a subset of molecules exist within an H-aggregate. Following initial excitation, the excitons that are generated on unaggregated molecules can then undergo energy migration to aggregated molecules that have increased conjugation length and therefore exist at lower energy. At low temperature however, this energy migration process is hindered, with relatively more emission occurring from unaggregated molecules from which fluorescence from the 0–0 transition is significantly stronger.

For completeness, we have measured the fluorescence decay lifetime of PF3T thin films at room temperature. In particular, we have recorded the fluorescence decay lifetime at 500 nm (close to the weakened transition at 507 nm) and at 550 nm. From our best fit to the data (after deconvoluting the TCSPC-system response function), we find that the decay lifetime at 500 nm is 112 ± 9 and 124 ± 16 ps at 550 nm. The similarity between these decay lifetimes suggests that in PF3T thin films, emission is dominated by the decay from a single molecular species, namely weakly coupled molecular H-aggregates.

B. Single Molecule Spectroscopy. When dispersed at sufficiently low concentration in an appropriate matrix polymer we can use single molecule spectroscopy techniques (SMS)^{34–37} to

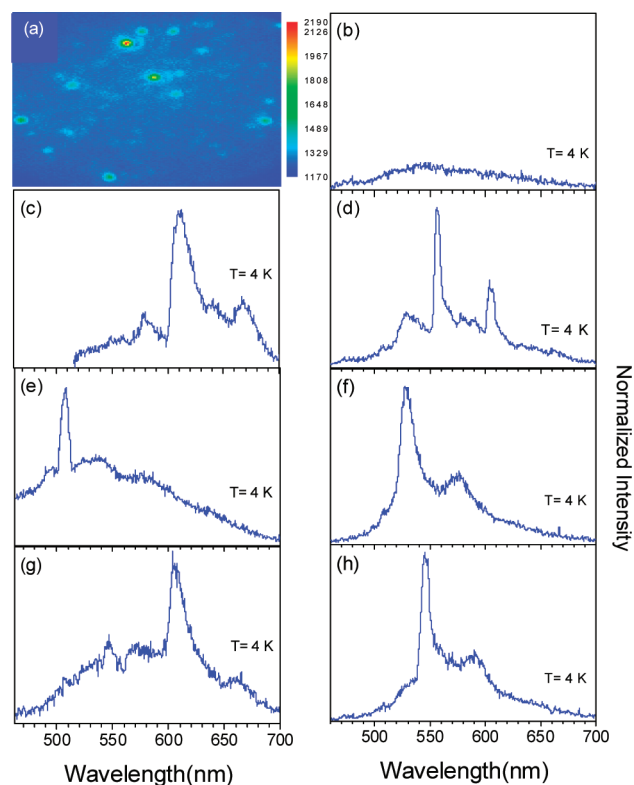


Figure 5. (a) Typical $20 \times 20 \mu\text{m}$ real-space image of PF3T emission when dispersed in a Zeonex matrix at a concentration of 5 ng L^{-1} . Part b shows the luminescence background emitted from a control film of Zeonex on a silver mirror at 4 K. Parts c–h show PF3T emission spectra recorded (at 4 K) from a series of emission spots as exemplified in part a.

investigate the PL emission from isolated PF3T molecules. Here, molecules are assumed to be separated from one another by a distance greater than the resolution limit of the microscope used to image the thin film.

Figure 5a shows a typical example of real-space fluorescence emission recorded from a thin film of PF3T in a Zeonex matrix at a concentration of $0.1 \mu\text{g L}^{-1}$ using our setup. Here, individual emissive spots can be resolved at surface density of $0.02 \mu\text{m}^{-2}$. To check whether these fluorescent spots correspond to emission from single molecules, their fluorescence spectra were measured at 4 K as shown in Figure 5c–h. To confirm that these emission features originate from PF3T, we also performed a series of control measurements in which we attempted to generate luminescence from thin films of the Zeonex matrix polymer coated onto a silver mirror. Figure 5b shows a typical spectrum, which it can be seen is characterized by a broad emission band that is at least 7 times weaker than the peak emission intensity from films containing PF3T dispersed in Zeonex. The origin of this weak background luminescence is at present unclear, nevertheless its broad line width and low intensity permits us to firmly associate the features observed in Figure 5c–h with PF3T.

We find approximately 5% of the bright emitting “spots” (as shown in Figure 5a) are characterized by a single emission peak observed at $(508 \pm 2) \text{ nm}$ that we believe corresponds to the 0–0 emission of a single chromophore on an isolated PF3T molecule. An example of such an emission spectrum is shown in Figure 5e. It is clear however that the fluorescence spectra of the majority of PF3T “spots” are usually composed of a number of relatively broader

features, suggesting that they most probably correspond to emission from multiple emitting-chromophores along a single molecular chain or emission from two or more loosely entangled chains. It appears however that a number of molecules are characterized by emission from a single red-shifted peak (such as Figure 5g) or by a vibrational progression in which the 0–0 transition is either broadened and red-shifted (Figure 5d), or extremely weak (Figure 5h), suggesting that in these cases we are again observing emission from molecular aggregates corresponding to two or more molecules that are dominated by H-aggregation. We believe that intramolecular aggregation (at the level of a single chain) is unlikely in this material due to its relatively low molecular weight.

It can be seen that emission from some of the emitting spots studied (e.g., see the spectra shown in Figure 5e) suggest emission from a single molecule having a Huang–Rhys parameter of almost zero. This is significantly smaller than the Huang–Rhys parameter determined for PF3T in solution at room temperature at low concentration (see Figure 4a) that has a value of around 0.65. The Huang–Rhys parameter provides a measurement of the extent to which the molecules can undergo conformational changes when in an excited state. Thus differences between the two sets of spectra can be anticipated from the fact that molecules in solution are more able to undergo a conformational changes compared to molecules dispersed in a (solid) Zeonex matrix at 4 K. The low temperature employed to record the single molecule emission spectra presented in Figure 5 also acts to “freeze” out librational and rotational modes of the molecules that contribute to line width broadening. Despite such effects however, the average (ensemble) emission spectra from PF3T molecules at low concentration in a matrix at low temperature is not significantly dissimilar from that recorded in a low concentration solution at room temperature (e.g., compare low concentration spectra presented in Figure 4 parts a and c). We conclude therefore that a relatively small fraction of single molecules are characterized by very a small Huang–Rhys factor.

The narrowest emission features observed in this study had a line width of $\sim 10 \text{ nm}$ ($\sim 45 \text{ meV}$) at 4 K (see Figure 5e); a value over 3 times narrower than the width of the 0–0 peak in Figure 3a. In general, we observe relatively narrow emission peaks at the short-wavelength end of the PF3T fluorescence spectra. Such linewidths are narrower than those measured from F8BT and PFR single molecules,¹⁴ however they are larger than the values observed for the polymer poly[2-methoxy-5-(2'-ethyl-hexyloxy)-p-phenylene vinylene] (MEH-PPV) where values between 2.5 meV ³⁴ and $13 \mu\text{eV}$ ^{35,36} have been reported. The relative broadness of the features observed in our spectra most probably results from spectral diffusion that occurs over a time-scale that is shorter than the integration time (30 s) used to collect our spectra. Such spectral diffusion processes are anticipated to result from thermally induced variations in the ground-state conformation of the molecule, changes in the polarizability of the surrounding polymer matrix or the presence of free charge.

Interestingly we have on a number of instances observed a significantly sharper peak (1 to 4 nm width) positioned at 506 nm (data not presented). Despite its proximity to the assumed 0–0 transition of PF3T we believe that it has a different origin; namely a Raman mode of the Zeonex matrix. To investigate this, we recorded a Raman spectrum of Zeonex on a silver mirror as shown in Figure 3c. It can be seen that there are a group of modes visible from 350 to 375 meV that are characteristic of $\text{sp}^3 \text{ C-H}$ stretch modes and a mode at 385 meV that corresponds to an $\text{sp}^2 \text{ C-H}$ stretch mode.^{38,39} In our spectroscopy measurements, we use a 442 nm laser, and thus the sharp peak observed at 506 nm lies at 354 meV below that of the

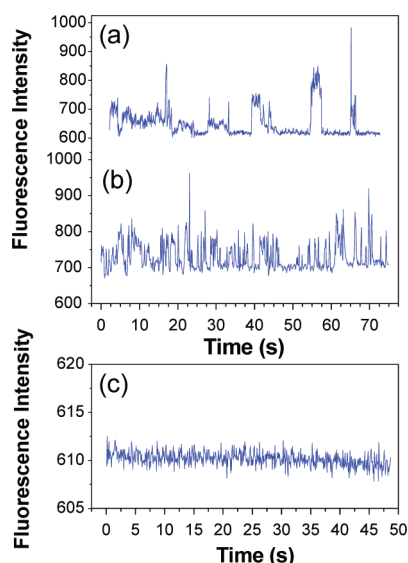


Figure 6. Fluorescence intensity transients of three PF3T emission spots recorded at room temperature under continuous wave excitation at 442 nm.

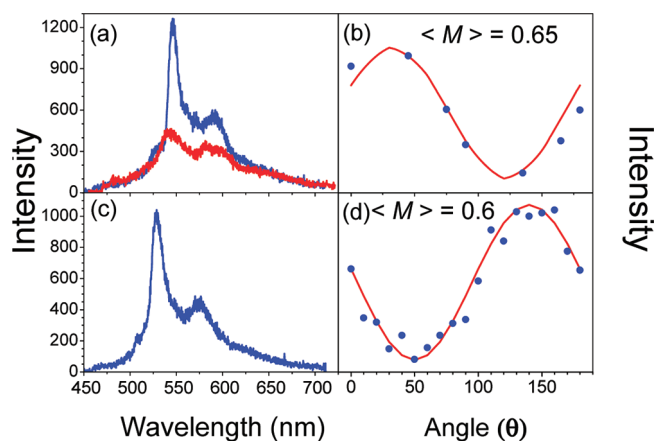


Figure 7. Part a shows the fluorescence intensity of a single emissive “spot” where the polarization of the laser has been fixed, but the relative angle of a polarizer placed in front of the monochromator is adjusted to give either maximum or minimum emission intensity. The fluorescence intensity observed from the same emissive spot as a function of the polarizer angle θ is shown in part b together with a fit to the data (see text for more details). Part c shows the fluorescence intensity of a single emissive “spot” (at fixed detection polarization) whose integrated emission intensity is plotted in part d as a function of the relative polarization of the excitation laser.

laser; an energy approximately coincident with the Raman mode at 356 meV. We also note that Baldini et al.⁴⁰ observed a relatively sharp peak at 778 nm in their fluorescence spectra of a Zeonex matrix, a wavelength that also corresponds to vibrational energy of 360 meV below the 635 nm laser diode used in their experiments. We have therefore excluded spectra that contain such a sharp emission peak at 506 nm from our data set.

To explore whether the emissive features identified in Figure 5a correspond to single molecules, we have followed the emission intensity of a series of emissive “spots” as a function of time at room temperature. Here, typical data is presented in

Figure 6a–c for three different emitting spots. It can be seen that the emission shown in parts a and b undergoes a characteristic blinking behavior above an average background intensity of 550 cps. Similar behavior has been seen in the polymer MEH-PPV and has been explained as resulting from fast localization of the excitation energy on one or a small number of chromophores.⁴¹ The emission from one “spot” however, shown in part c, is effectively constant, suggesting it either corresponds to an intermolecular aggregate on which emission occurs from a number of uncorrelated chromophores or a molecule having a larger than average molecular weight on which a number of uncorrelated chromophores are emitting.

We have also measured both the absorption and emission polarization of the emissive spots to explore the extent to which we are observing single chromophores on isolated PF3T molecules. Figure 7a shows an example of an emission spectrum recorded from a single spot where the polarization of the laser has been fixed, but the relative angle of a polarizer placed in front of the monochromator is varied. Here two spectra are presented corresponding to the maximum and minimum emission intensity of the molecule as a function of polarizer angle in part b. Following refs 14 and 42, we can fit the angular emission intensity $I(\theta)$ to

$$I(\theta) = I_0(1 + M \cos(2(\theta - \phi))) \quad (1)$$

where M is the absorption anisotropy, ϕ is a phase angle and I_0 is a fitting constant. The emitter whose emission spectrum is shown in Figure 7(a) has an apparent emission anisotropy of 0.65. This relatively low anisotropy confirms that we are most probably observing emission from more than one chromophore. It can be seen for this emitter that the peak at 545 nm apparently has a greater emission anisotropy than does the peak at 595 nm, as it undergoes a greater reduction in intensity between the two orthogonal polarizations. This suggests that the two emission features are not well correlated and may correspond to the emission from independent states.

We have also recorded the absorption anisotropy of various emitting spots. This was performed fixing the detection polarization and recording the wavelength integrated emission intensity as a function of excitation laser polarization. An example of this is shown in Figure 7, parts c and d, where we plot the emission spectrum from a typical spot and its emission intensity as a function of laser polarization respectively. In this case, we calculate an anisotropy of 0.6. From the ~ 30 molecules we have studied, we determine an average anisotropy value of $\langle M \rangle = 0.65 \pm 0.04$. Out of 27 PF3T emitters examined, two had a zero or near zero absorption anisotropy, indicating that they are most likely an aggregate consisting of a number of entangled or otherwise associated molecular chains. Notably however, a small number of PF3T emitters had a high polarization anisotropy (>0.85) confirming that they most probably correspond to emission from a single chromophore. In general, we find that such molecules having higher emission polarization anisotropy are also characterized by narrower emission linewidths.

IV. CONCLUSIONS

We have studied the optical properties of PF3T in bulk films, in solution, and when dispersed in a polynorbornene matrix polymer as a function of molecular concentration and excitation wavelength. The results of this study imply the formation of weakly interacting H-aggregates at high concentration, in both

thin-film and solution which suppresses emission from the 0–0 (electronic) transition. This transition becomes stronger as the PF3T concentration is reduced. At sufficiently low concentration, aggregate formation is relatively suppressed and more “intrinsic” single molecule emission is observed. Our measurements confirm other studies that show that intermolecular interactions in both polymers and oligomers can play an important role in determining both electronic and optical properties.

On diluting PF3T molecules in an inert matrix, we have been able to identify emission from single PF3T chromophores that we show is characterized by a single relatively narrow (45 meV) peak at 4 K located at 508 ± 2 nm. To confirm the identification of single chromophore emission, we have also recorded emission intensity as a function of time from a number of localized emitters. We show that some emitters undergo a characteristic “blinking” and switch from a dark to a light state over a period of hundred milliseconds, indicating that emission is dominated by a small number of emissive chromophores. We find however that many spectra detected from PF3T dispersed in a Zeonex matrix at low concentration probably correspond to emission from multiple chromophores emitting from single molecular chain or from π -stacked molecules or loosely associated intermolecular aggregates.

■ ASSOCIATED CONTENT

S Supporting Information. Figure S1 showing the Huang–Rhys factor of PF3T as a function of concentration in solution and in thin film. Figure S2 showing the normalized photoluminescence emission spectra of a PF3T thin film as a function of temperature from room temperature to 4 K. This material is available free of charge via the Internet at <http://pubs.acs.org>.

■ AUTHOR INFORMATION

Corresponding Author

*E-mail: d.g.lidzey@sheffield.ac.uk. Tel: +44 (0)114 222 3501. Fax: +44 (0)114 222 3555.

Present Addresses

*Department of Physics, University of Hull, Cottingham Road, Hull HU6 7RX, United Kingdom.

Notes

[†]E-mail: G.khalil@sheffield.ac.uk.

■ ACKNOWLEDGMENT

This work was supported by the UK EPSRC through Grant No. EP/D064767/1 ‘Nano-Scale Organic Photonic Structures’ and via a research grant from Murata Ltd. We thank Stuart Harris at Zeon Chemicals Europe Ltd. for the gift of the Zeonex polymer. We gladly thank Alex Thiessen and John Lupton at the University of Utah and Jenny Clark at the University of Cambridge for many useful and enlightening discussions.

■ REFERENCES

- (1) Burroughes, J. H.; Bradley, D. D. C.; Brown, A. R.; Marks, R. N.; Mackay, K.; Friend, R. H.; Burns, P. L.; Holmes, A. B. *Nature* **1990**, *347*, 539.
- (2) Yang, Y.; Heeger, A. J. *Nature* **1994**, *372*, 344.
- (3) Nguyen, L. H.; Hoppe, H.; Erb, T.; Günes, S.; Gobsch, G.; Sariciftci, N. S. *Adv. Funct. Mater.* **2007**, *17*, 1071.
- (4) Chen, L.; McBranch, D. W.; Wang, H.-L.; Helgeson, R.; Wudl, F.; Whitten, D. G. *Proc. Natl. Acad. Sci. U.S.A.* **1999**, *96*, 12287.
- (5) Charas, A.; Morgado, J.; Martinho, J. M. G.; Alcacer, L.; Cacialli, F. *Chem. Commun.* **2001**, 1216.
- (6) Charas, A.; Morgado, J.; Martinho, J. M. G.; Alcacer, L.; Cacialli, F. *Synth. Met.* **2002**, *127*, 251.
- (7) Charas, A.; Morgado, J.; Martinho, J. M. G.; Fedorov, A.; Alcacer, L.; Cacialli, F. *J. Mater. Chem.* **2002**, *12*, 3523.
- (8) Charas, A.; Morgado, J.; Martinho, J. M. G.; Alcacer, L.; Lim, S. F.; Friend, R. H.; Cacialli, F. *Polymer* **2003**, *44*, 1843.
- (9) Charas, A.; Alves, H.; Martinho, J. M. G.; Alcacer, L.; Fenwick, O.; Cacialli, F.; Morgado, J. *Synth. Met.* **2008**, *158*, 643.
- (10) Burrows, H. D.; Arnaut, L. G.; Pina, J.; Seixas de Melo, J.; Chattopadhyay, N.; Alcacer, L.; Charas, A.; Morgado, J. *Chem. Phys. Lett.* **2005**, *402*, 197.
- (11) Meskers, S. C. J.; Janssen, R. A. J.; Haverkort, J. E. M.; Wolter, J. H. *Chem. Phys.* **2000**, *260*, 415.
- (12) Spano, F. C. *J. Chem. Phys.* **2005**, *122*, 234701.
- (13) Clark, J.; Silva, C.; Friend, R. H.; Spano, F. C. *Phys. Rev. Lett.* **2007**, *98*, 206406.
- (14) Khalil, G. E.; Adawi, A. M.; Fox, A. M.; Iraqi, A.; Lidzey, D. G. *J. Chem. Phys.* **2009**, *130*, 044903.
- (15) Winokur, M. J.; Cheun, H.; Knaapila, M.; Monkman, A. P.; Scherf, U. *Phys. Rev. B* **2007**, *75*, 113202.
- (16) Zeng, L.; Yan, F.; Wei, S.K.-H.; Culligan, S. W.; Chen, S. H. *Adv. Funct. Mat.* **2009**, *19*, 1978.
- (17) Liedtke, A.; O'Neill, M.; Kelly, S. M.; Kitney, S. P.; Averbek, B. V.; Boudard, P.; Beljonne, D.; Cornil, J. *J. Phys. Chem. B* **2010**, *114*, 11975.
- (18) Chen, S.-H.; Su, A.-C.; Huang, Y.-F.; Su, C.-H.; Peng, G.-Y.; Chen, S.-A. *Macromolecules* **2002**, *35*, 4229.
- (19) Chen, S. H.; Su, A. C.; Chou, H. L.; Peng, K. Y.; Chen, S. A. *Macromolecules* **2004**, *37*, 167.
- (20) Narwark, O.; Meskers, S. C. J.; Peetz, R.; Thorn-Csányi, E.; Bäessler, H. *Chem. Phys.* **2003**, *294*, 1.
- (21) Ho, P. K. H.; Kim, J.-S.; Tessler, N.; Friend, R. H. *J. Chem. Phys.* **2001**, *115*, 2709.
- (22) Svedberg, F.; Alaverdyan, Y.; Johansson, P.; Käll, M. *J. Phys. Chem. B* **2006**, *110*, 25671.
- (23) Louarn, G.; Trznadel, M.; Buisson, J. P.; Laska, J.; Pron, A.; Lapkowski, M.; Lefrant, S. *J. Phys. Chem.* **1996**, *100*, 12532.
- (24) Khan, A. L. T.; Banach, M. J.; Köhler, A. *Synth. Met.* **2003**, *139*, 905.
- (25) Brown, P. J.; Thomas, D. S.; Köhler, A.; Wilson, J. S.; Kim, J.-S.; Ramsdale, C. M.; Sirringhaus, H.; Friend, R. H. *Phys. Rev. B* **2003**, *67*, 064203.
- (26) Thomas, S.; Venkateswaran, S.; Kapoor, S.; D'Cunha, R.; Mukherjee, T. *Spectrochim. Acta Part A: Molec. Biomolec. Spect.* **2004**, *60*, 25.
- (27) Sarkar, U. K.; Chakrabarti, S.; Misra, T. N.; Pal, A. *J. Chem. Phys. Lett.* **1992**, *200*, 55.
- (28) Tsoi, W. C.; Lidzey, D. G. *J. Phys.: Condens. Matter* **2008**, *20*, 125213.
- (29) Ariu, M.; Lidzey, D. G.; Bradley, D. D. C. *Synth. Met.* **2000**, *111–112*, 610.
- (30) Harrison, N. T.; Baigent, D. R.; Samuel, I. D. W.; Friend, R. H.; Grimsdale, A. C.; Moratti, S. C.; Holmes, A. B. *Phys. Rev. B* **1996**, *53*, 15815.
- (31) Guha, S.; Rice, J. D.; Yau, Y. T.; Martin, C. M.; Chandrasekhar, M.; Chandrasekhar, H. R.; Guentner, R.; Scanducci de Freitas, P.; Scherf, U. *Phys. Rev. B* **2003**, *67*, 125204.
- (32) Kim, Y.; Cook, S.; Tuladhar, S. M.; Choulis, S. A.; Nelson, J.; Durrant, J. R.; Bradley, D. D. C.; Giles, M.; McCulloch, I. H.; C.-S.; Ree, M. *Nat. Mater.* **2006**, *5*, 197.
- (33) Ariu, M.; Lidzey, D. G.; Sims, M.; Cadby, A. J.; Lane, P. A.; Bradley, D. D. C. *J. Phys.: Condens. Matter* **2002**, *14*, 9975.
- (34) Schindler, F.; Lupton, J. M. *ChemPhysChem* **2005**, *6*, 926.
- (35) Feist, F. A.; Tommaseo, G.; Basche, T. *Phys. Rev. Lett.* **2007**, *98*, 208301.

- (36) Feist, F. A.; Basche, T. *J. Phys. Chem. B* **2008**, *112*, 9700.
- (37) Schindler, F.; Lupton, J. M.; Feldmann, J.; Scherf, U. *Adv. Mater.* **2004**, *16*, 653.
- (38) Parker, S. F.; Williams, K. P. J.; Steele, D.; Herman, H. *Phys. Chem. Chem. Phys.* **2003**, *5*, 1508.
- (39) Kawai, N. T.; Butler, I. S.; Gilson, D. F. R. *J. Phys. Chem.* **1990**, *95* (2), 634.
- (40) Baldini, F.; Carloni, A.; Giannetti, A.; Porro, G.; Trono, C. *Sens. Actuators, B* **2009**, *139*, 64.
- (41) Ebihara, Y.; Vach, M. *J. Phys. Chem. B* **2008**, *112* (40), 12575.
- (42) Hu, D.; Yu, J.; Padmanaban, G.; Ramakrishnan, S.; Barbara, P. F. *Nano Lett.* **2002**, *2*, 1121.